Initial proof-of-principle for near room temperature Xe and Kr separation from air with MOFs

Fuel Cycle Research & Development

Prepared for
U.S. Department of Energy
Campaign or Program
PK Thallapally and DM Strachan
Pacific Northwest National Laboratory
June 6, 2012
FCRD-SWF-2012-000131
PNNL-21452

SUMMARY

Materials were developed and tested in support of the U.S. Department of Energy's Office of Nuclear Energy, Fuel Cycle Technology Separations and Waste Forms Campaign. Specifically, materials are being developed for the removal of xenon (Xe) and krypton (Kr) from gaseous products of nuclear fuel treatment.

During fiscal year 2012, three metal organic framework (MOF) structures were investigated in greater detail for the removal and storage of Xe and Kr from air at room temperature. Breakthrough measurements on a nickel-based MOF indicate this material could capture and separate parts per million by volume (ppmv) levels of Xe (400 ppmv) from air (40 ppmv Kr, 78% N_2, 21% O_2, 0.9% Ar, and 0.03% CO_2). Similarly, the selectivity of a fluorinated MOF can be changed from Xe > Kr to Xe < Kr simply by changing the temperature over a narrow range (-30 °C). Estimates were made for the cost of bulk quantities of MOFs and compared to other capture materials.

CONTENTS

FIGURES

TABLES

ACRONYMS

CPHFP	2,20-bis(4-carboxyphenyl)hexafluoropropane
FMOFCu	Fluorinated Metal Organic Framework with Cupper clusters
GCMC	grand canonical Monte Carlo
HKUST-1	Hong Kong University of Science and Technology based MOF
MOF	metal organic framework
Ni/DOBDC	Nickel Dioxobenzenedicarboxylic ac
sccm	standard cubic centimeters per minute
THF	Tetrahydrofuran
XRD	X-ray diffraction
ZIF	zeolite imidazolate frameworks

INITIAL PROOF-OF-PRINCIPLE FOR NEAR ROOM TEMPERATURE XE AND KR SEPARATION FROM AIR WITH MOFS

1. INTRODUCTION

During reprocessing, fission-product gases are released when the fuel cladding is breached and when the fuel is reacted (such as in voloxidation and dissolution). Two of these gases are xenon (Xe) and krypton (Kr). Both Xe and Kr have radioactive isotopes, most of which are short lived ($t_{1/2}$ < 40 d) and two have longer-lived isotopes (^{81}Kr [$t_{1/2} = 2.1 \times 10^5$ y] and ^{85}Kr [$t_{1/2}$ = 10.7 y]). Of these, ^{85}Kr is the isotope of concern for the inert gas fission products. In an operating reprocessing plant, ^{85}Kr is diluted with air and must be separated before the air is released through the stack. Separating ^{85}Kr from air is complicated by the presence of Kr in air, the nonradioactive Xe from the fuel, and the low concentrations of both inert gases.

The two developed processes to remove Xe and Kr from nuclear fuel treatment off-gas both require cryogenically cooled the air and removal of air components, leaving behind a mixture of Xe and Kr and possibly argon (Ar) with nitrogen – cryogenic distillation and cryogenic adsorption (Eby et al. 1982; Henrich and Weirich 1989). Installing a cryogenic process and its operation is very expensive and energy intensive. Thus, a process to remove these gases at much higher temperatures would be advantageous and cost effective, especially if the process could operate at close to ambient conditions. Zeolites and activated carbons have been tested for Xe and Kr separation with selectivities of approximately four to six with very low capacities (0.5 - 2 mmol/g) (Jameson et al. 1997; Bazan et al. 2011; Munakata et al. 2003).

In this document, metal organic framework (MOF) materials are described that offer the possibility of removing Xe and Kr from air and from each other at near room temperature and at high capacity. MOF materials represent a new class of functional materials consisting of metal centers linked with organic building blocks to produce diverse and customizable structural frameworks (Eddaoudi et al. 2002; Liu et al. 2012; Sanchez et al. 2011; Perry et al. 2009; Farha and Hupp 2010). These materials could augment the existing technology for the storage of ^{85}Kr in addition to the possibility of removing Xe and Kr from air at elevated temperatures -- Kr is isolated in a MOF cage. One main issue with storage of ^{85}Kr in stainless-steel canisters at elevated pressures is the decay product rubidium (Rb). Rb is a corrosive liquid at projected ^{85}Kr storage temperatures. The use of MOFs augments this technology in two ways. First, it allows more gas to be stored in the canister at lower pressures. Secondly, the decay product Rb would be isolated from the metal canister, thereby reducing the corrosion concerns. In addition, if there is sufficient specificity that Xe and Kr could be separated from each other, then the inert Xe—the mass of which is 15 times that of ^{85}Kr—would not need to be stored. Recent cost estimates indicate MOFs have comparable costs when produced in bulk as other adsorbents; see Section 4 (Liu et al. 2012).

Although research to date is limited regarding noble gas adsorption, storage of these gases was demonstrated with some MOFs (Mueller et al. 2006). Recently, the research team reported that a MOF known as Ni/DOBDC has a Xe capacity of 4.16 mol/kg at 1 bar and 298 K, which is higher than that of a charcoal carbon (Thallapally et al. 2012). Greathouse et al. (2009) used grand canonical Monte Carlo (GCMC) simulation to investigate Xe and Kr separation in a MOF known as IRMOF-1. Ryan and Snurr et al. (2011) simulated Xe and Kr separation with several other MOFs with GCMC. In other simulations, work on screening the Xe and Kr selectivity for 137 000 hypothetical MOFs has also recently been published by (Ryan et al. 2011). Ryan et al (2011) found that the MOFs with polar functional groups tend to have higher Xe selectivities compared to those without polar functional groups. Moreover, the Xe selectivity was maximized when the MOF structures had pore morphologies resembling tubes of uniform

pore diameter. However, no experimental studies have been reported in the literature to date on the removal of Xe and Kr from air with MOFs.

In this report, the research team assessed MOFs for use in removing Xe and Kr from air at ambient conditions.

1.1 Basis for Metal Organic Framework Selection

Three benchmark MOFs—Ni/DOBDC, HKUST-1 and FMOFCu shown in Figure 1—were studied for Xe and Kr adsorption with a dynamic breakthrough column method. These MOFs were selected for several reasons. First, all MOFs contain unsaturated metal centers, which are polar sites and estimated to be favorable for Xe and Kr adsorption. Second, the Ni/DOBDC is known to have high hydrothermal stability (Eddaoudi et al. 2002; Liu 2012; Sanchez et al. 2011; Thallapally et al. 2012) and higher Xe capacity than activated carbon. Third, the HKUST-1 has small aperture pores (0.5 nm) and pores with a larger diameter (15 nm) in the center, while the Ni/DOBDC has a uniform, 11-nm cylindrical pore. Investigating the effects of pore morphology on Xe and Kr selectivity for MOFs was interesting, both experimentally and theoretically.

An important feature of FMOFCu is that 0.5 × 0.5-nm tubular cavities are connected through small (bottleneck) windows (0.35 × 0.35 nm) as shown in Figure 1. Although FMOFCu cages have a larger size than the kinetic diameters of Xe and Kr (0.396 nm and 0.360 nm, respectively), the research team selected this material because the connecting windows have dimensions practically similar (based on atom to atom distances) to the kinetic diameter of Kr and are smaller than the corresponding Xe diameter. Therefore, Xe diffusion into the cavities should be restricted; thus, FMOFCu should be more selective for Kr *via* molecular sieving than NiDOBDC and HKUST-1 where the connecting windows are much larger than the kinetic diameters of Xe or Kr.

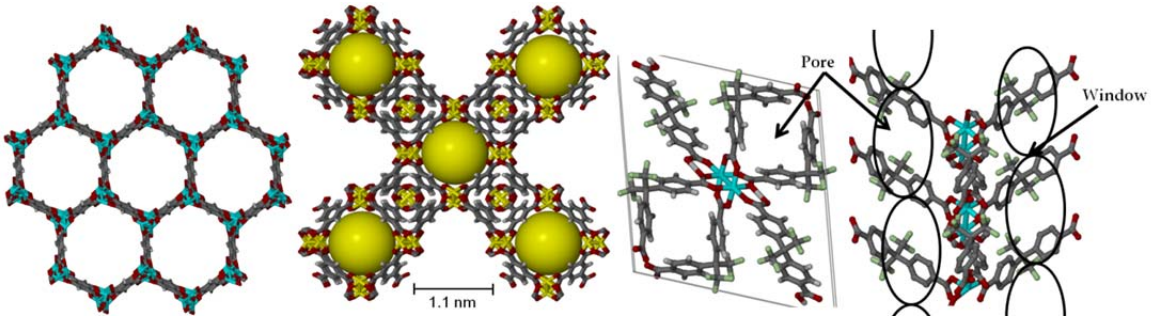

Figure 1. Crystal structures for MOFs after removing solvent molecules. Left: Ni/DOBDC; middle: HKUST-1; and right: FMOFCu.

1.1.1 Materials Synthesis and Preparation

The Ni/DOBDC was synthesized following a procedure reported in the literature (Bonino et al. 2008). Briefly, a solution of 2,5 dihydroxyterephthalic acid (1.486 g, 7.5 mmol) in THF (25 mL) and a solution of nickel (II) acetate tetrahydrate (3.733 g, 15 mmol) in water (25 mL) were combined in a Teflon®-lined, 100 mL stainless-steel pressure vessel. The reaction was conducted for 3 days at 110 °C. Filtration yielded 3.169 g of a yellowish, fine crystalline product that was washed three times with water (50–100 mL) and dried in air at 85 °C under vacuum. The HKUST-1 was purchased from Sigma-Aldrich and used as is. For comparison, the research team purchased USFilter AquaCarb® 1230C coconut shell activated carbon in 1–2 mm pellets.

The synthesis of FMOFCu was performed following a similar procedure. Copper nitrate trihydrate ($Cu(NO_3)_2 \cdot 3H_2O$ (99% from Aldrich Chemicals) and 2,20-bis(4-carboxyphenyl)hexafluoropropane (CPHFP) (99% from Matrix International) were used as received without further purification. Crystals of FMOFCu were obtained by a hydrothermal reaction of $Cu(NO_3)_2 \cdot 3H_2O$ (0.024 g, 0.1 mmol) with an excess of CPHFP (0.122 g, 0.31 mmol) in 5 mL of deionized water at 150 °C for 12 h. The molar ratio of the reaction was 1:3:2778. Excess CPHFP was removed by repeatedly washing the product with 10 mL of N,N-dimethylformamide (DMF), followed by drying the product in air for an hour.

To minimize pressure drop and prevent potential contamination to the instrument, MOF pellets were used for the breakthrough experiments. The Ni/DOBDC and HKUST-1 pellets were formed through two steps. First, a powder sample with no binder was pressed into a disk under 12 MPa for 5 minutes. Then, the disk was carefully broken and the fragments were sieved for a 20–30 mesh (600–850 μm) fraction. This two-step process was repeated to make sufficient pellets for the experiment. Surface areas for the pellet samples are reported in Appendix A (Figure A2); results show the surface areas of the pellets decreased slightly compared to the powder samples for MOFs. However, gas adsorption properties for the pellet samples are similar to their powder predecessors.

Pure helium (He), Xe, and Kr gases were purchased from OXARC, Inc. (Spokane, Washington) without further purification. The low concentration Xe and Kr mixtures in air were also purchased from OXARC Inc. with certified Xe and Kr concentrations according to the research team's requirements.

1.1.2 Test Bed for Evaluating Xe and Kr Capture with MOFs

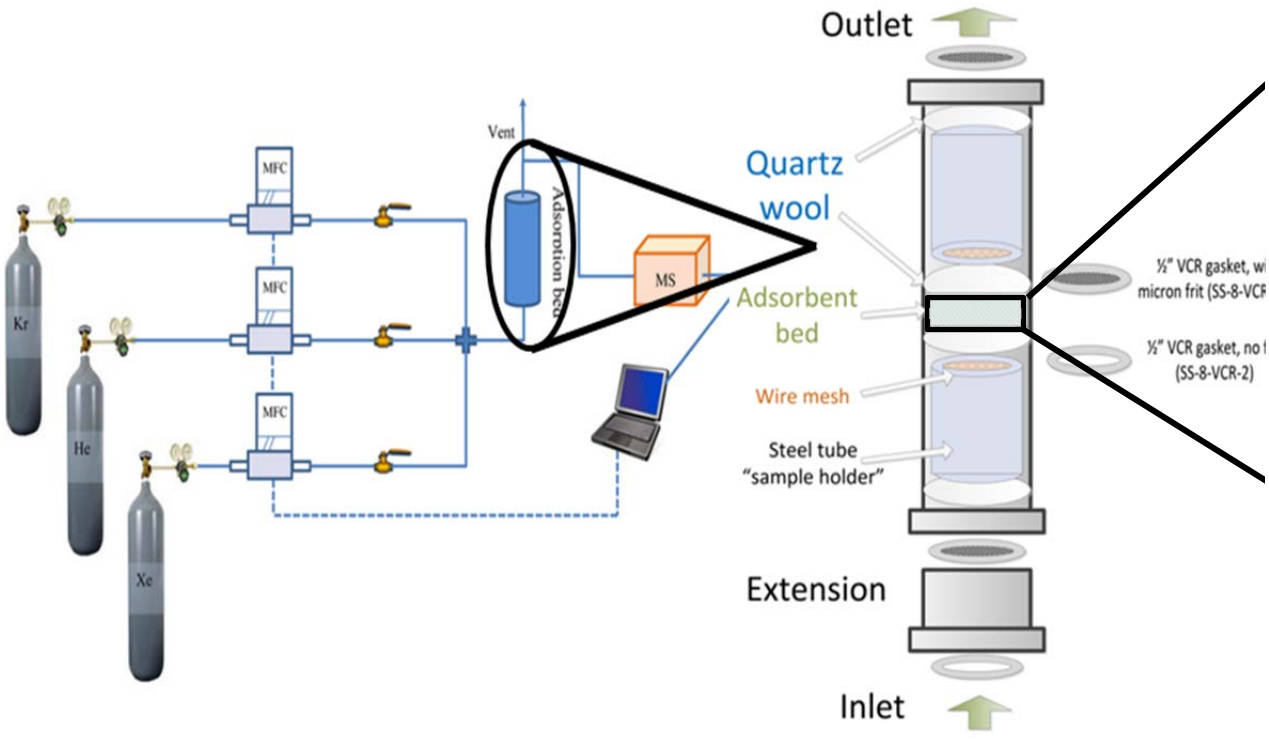

Figure 2. Schematic of Xe and Kr breakthrough experiment apparatus. Illustration shows the loading of samples in the adsorption reactor for breakthrough experiments.

The Xe and Kr breakthrough curves were measured for the Ni/DOBDC and HKUST-1 in a dynamic sorption analyzer (ARBC, Hiden Analytical Ltd., Warrington, UK.) shown in Figure 2. Prior to gas adsorption experiments, the samples were regenerated by heating at certain temperatures in situ under He purge for 15 h. The sample was purged with He before and again after Xe and Kr breakthrough experiments. This procedure is used with all the tested samples. In a typical pure Xe and Kr breakthrough experiment, a gas mixture with a total flow rate of 0.42 mL/s (25 standard cubic centimeters per minute [sccm]) and a total pressure of 1 bar flows through the adsorption bed. For a Kr and Xe mixture, a total flow rate of 0.84 mL/s and a total pressure of 1 bar was used. Similarly, for the separation of Xe (1000 ppmv Xe in air) and Kr (1000 ppmv Kr in air) from air, a flow rate of 0.33 mL/s at 1 bar was used. The same setting was also applied to a separation of Xe (400 ppm) and Kr (40 ppm) mixture from air.

The sample was loaded in two layers of quartz wool (Figure 2). The bed aspect ratio is about 3:4. Gases are introduced through the bottom inlet of the adsorption bed. Frit gaskets are installed at both the top and bottom of the column to prevent any powder contamination to the instrument. The pressure drop caused by the frit gaskets is negligible. Powder X-ray diffraction (XRD) analyses were performed on a Bruker X-ray diffractometer (D8 FOCUS, Bruker AXS Inc., Madison, Wisconsin) with a diffracted beam monochromator, and a copper target X-ray tube set to 40 kV and 150 mA. Nitrogen adsorption experiments at -196°C were performed with an automatic gas sorption analyzer (Quantachrome Autosorb IQ, Quantachrome Instruments, Boynton Beach, Florida).

2. Results and Discussion

2.1 Pure Xenon and Krypton Breakthrough

Pure Xe and Kr breakthrough curves for the Ni/DOBDC sample are shown in Figure 3 (left). The retention time of Xe is clearly longer than that of Kr. Thus, the Ni/DOBDC can adsorb more Xe than Kr as expected. The Xe and Kr capacities for the Ni/DOBDC and other materials can be calculated by integrating the areas above the breakthrough curves as shown in Liu et al. (2012). The Xe and Kr dynamic capacities for NiDOBDC at 1 bar and 25 °C were calculated and are summarized in Figure 3 (right).

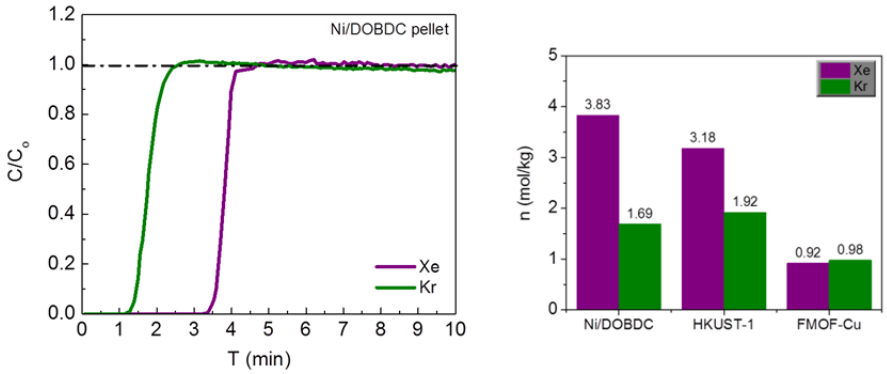

Figure 3. Pure Xe and Kr breakthrough curves for the Ni/DOBDC at 1 bar and 25 °C (left). Pure Xe and Kr breakthrough capacities for MOFs at 1 bar and 25 °C (right, compared with other MOFs).

The results for the Ni/DOBDC are in agreement with the pure gas isotherms obtained with a static method. Xenon is preferentially adsorbed on NiDOBDC over Kr because of larger polarizability of Xe. The Ni/DOBDC has the highest dynamic Xe capacity followed by HKUST-1 and FMOFCu. The Ni/DOBDC can adsorb more Xe but less Kr, which may indicate the Ni/DOBDC has a higher Xe/Kr selectivity.

2.2 Separation of Xenon and Krypton from Air

Experiments were conducted for separating low concentrations of Xe and Kr from air, which is important from a practical point of view. A total of 1000 ppmv Xe balanced with air (N_2: 78%, O_2: 21%, Ar: 0.9%, CO_2: 0.03%) and a total of 1000 ppmv Kr balanced with air were selected as two target gases to represent low concentrations of Xe and Kr in waste air streams. The results for the Ni/DOBDC and HKUST-1 are shown in Figures 4 and 5, respectively. Before the breakthrough experiments, the bed was purged with He for 10 minutes and then switched to the target gas mixtures.

For the Ni/DOBDC, N_2 and O_2 break through almost instantly while Xe remains in the adsorption bed for about 10 minutes, which is also longer than CO_2 (Appendix A, Figure A3). Kr appears to break through at a slightly longer time compared to N_2 and O_2. The Xe capacity for the Ni/DOBDC at 25 °C and 1000 ppmv was determined to be 9.3 mmol/kg (0.12 mass%) from the breakthrough method. Similarly, the Kr capacity for the Ni/DOBDC at 25 °C and 1000 ppm was determined to be 1.8 mmol/kg (0.015 mass%) from the breakthrough method. Again, Ni/DOBDC selectively adsorbs Xe over Kr as seen in Figure 4, but it appears the difference was enlarged at a low concentration because the Xe and Kr selectivity of the Ni/DOBDC increased to about 5.3 when the concentration of Xe was 1000 ppm.

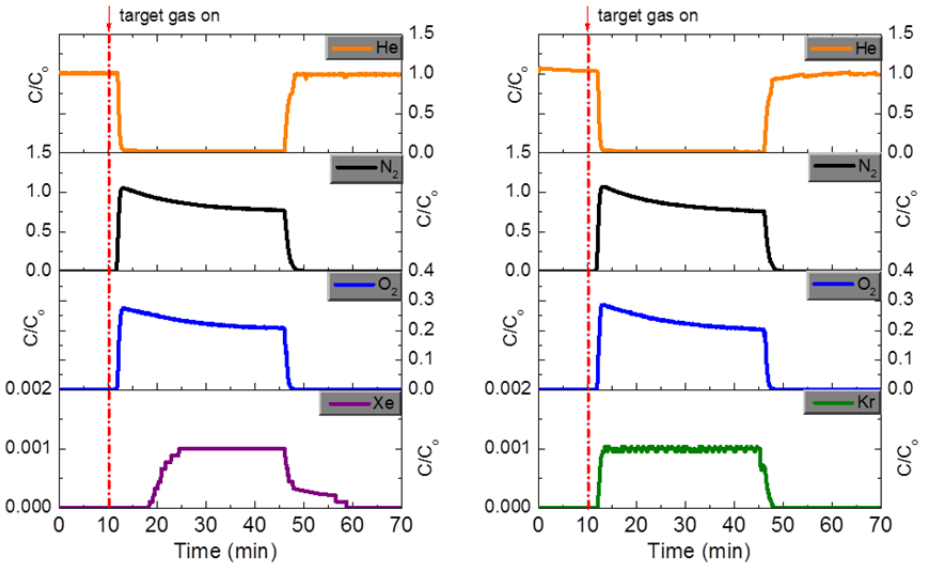

Figure 4. Xenon 1000 ppmv in air and 1000 ppmv Kr in air breakthrough curves at 25 °C for the Ni/DOBDC. The He flow rate is 20 sccm and the flow rates of Xe and Kr in air are also 20 sccm.

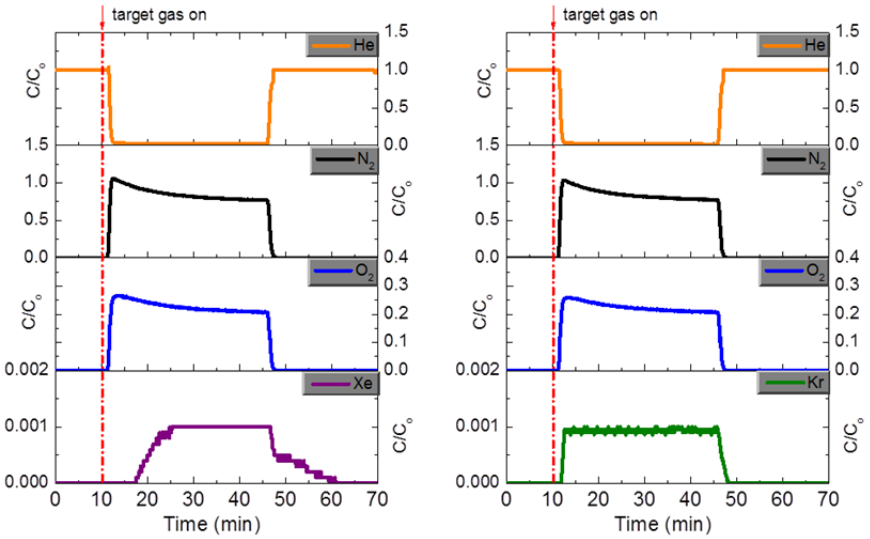

Figure 5. Xenon 1000 ppmv in air and Kr 1000 ppmv in air breakthrough curves at 25 °C for the HKUST-1. The He flow rate is 20 sccm and the flow rates of Xe and Kr in air are also 20 sccm.

The HKUST-1 (Figure 5) has a smaller Xe capacity (8.5 mmol/kg) but larger Kr capacity (2.0 mmol/kg) compared to the Ni/DOBDC at 25°C. Therefore, compared to HKUST-1, the Ni/DOBDC has a higher Xe capacity and a higher Xe and Ke selectivity, which is important for separating Xe from a mixture of Xe and Kr. The high Xe and Kr selectivity of Ni/DOBDC may be a result of the stronger interactions between the unsaturated metal centers and Xe atoms, which have higher polarizability than Kr atoms. In addition, the uniform cylindrical pore morphology of the Ni/DOBDC may be a factor in enhancing the Xe/Kr selectivity.

Finally, a mixture of low concentration Xe and Kr in air (Kr: 40 ppmv; Xe: 400 ppmv; N_2: 78%; O_2: 21%; Ar: 0.9%; CO_2: 0.03%) was chosen to simulate the separation of trace amount of Xe and Kr from the processed off-gas from a reprocessing plant with Ni/DOBDC. The breakthrough results are shown in Figure 6. Note the results reported are based on average signals for both Xe and Kr because of the low concentrations. According to the results, N_2 and O_2 have the shortest effluent times followed by CO_2 and Kr. The research team still noted a clear "roll-up" in the Kr breakthrough curve and the Kr concentration decreased significantly after the roll-up. Of importance is that Xe did not break through the bed until about 15 minutes after Kr and other components in air. The research team believes this is the first time experimental evidence has been provided to show MOF materials can successfully separate ppm level Xe from Kr mixtures in air. Similarly, the Xe and Kr capacities at 400 ppmv and 40 ppmv for the Ni/DOBDC are determined to be 4.8 mmol/kg and 0.066 mmol/kg, respectively. Thus, the Xe/Kr selectivity is estimated to reach about 7.3 for the Ni/DOBDC under these conditions.

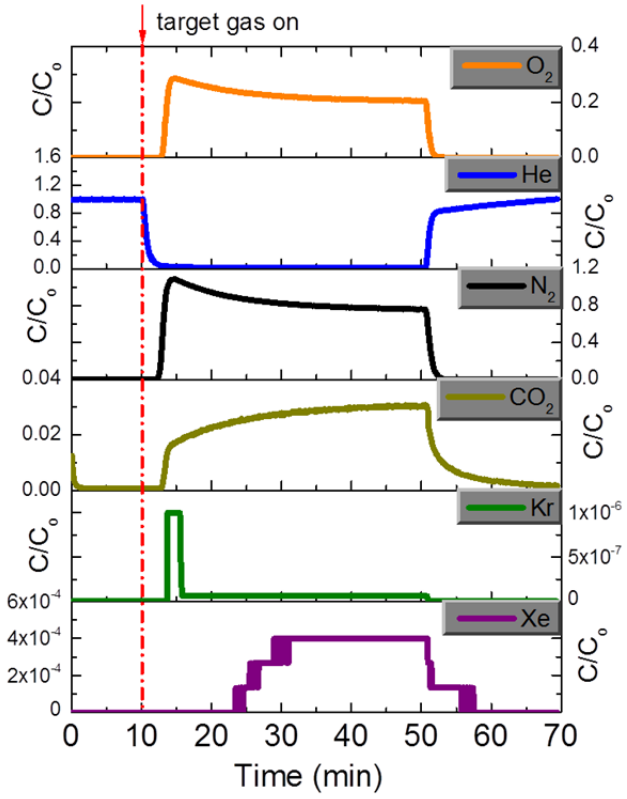

Figure 6. Xenon 400 ppmv and Kr 40 ppmv in air breakthrough curves at 25 °C for the Ni/DOBDC. The flow rates are 20 sccm.

3. FMOFCu

Pure Kr and Xe adsorption/desorption experiments were performed at different temperatures on FMOFCu. Figure 7 shows the adsorption isotherms for Kr and Xe at six different temperatures. The isotherms at each temperature show a gradual gain in uptake with pressure with no saturation at 1 bar. The adsorption values increase for both Kr and Xe as the temperature decreases, which is the expected behavior for most MOFs. Desorption profiles on FMOFCu indicate no obvious hysteresis for either Xe or Kr. A significant result is the faster increase in Kr uptake as the temperature is decreased as compared to Xe. Figure 7 shows that at room temperature, the capacity for Kr is comparable to the capacity observed for Xe at all pressures and the selectivity of FMOFCu toward these gases seems to revert at temperatures below room temperature; this was not observed for other MOFs. The inversion in Kr and Xe selectivity in FMOFCu was clearly observed in Figure 8 (left) where a graph of the sorption of Kr and Xe as a function of temperature is shown at 1 bar. The figure also shows a rapid increase in uptake for both gases; however, this increase (as described above) is faster for Kr. Furthermore, the adsorption of Xe at temperatures below 0ºC begins to decrease and reaches sorption values lower than that of 40 ºC. In addition, the Xe and Kr adsorption isotherms obtained at -40 ºC and 40 ºC further demonstrates the inversion in Kr and Xe selectivity. The Kr and Xe molar selectivity as a function of temperature (270 K to 313 K) was estimated from the pure gases isotherms (Figure 8). Clearly, the selectivity reverts at temperatures below room temperature and increases nearly exponentially with decreasing temperatures at 0.1 bar. At this pressure and temperature (203 K), the material shows an estimated Kr and Xe molar selectivity of 36 as compared to 0.45 at 40 ºC.

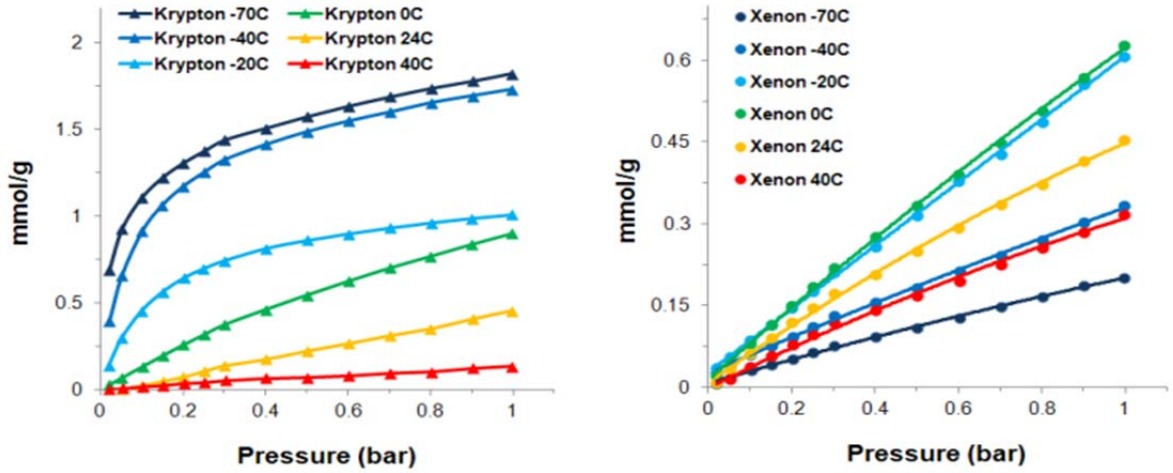

Figure 7. Xenon and krypton sorption isotherms for FMOFCu at different temperatures. Note the decrease in Xe uptake at temperatures below 0 ºC at all pressures.

This behavior is significant because it shows for the first time that a MOF reverses its selectivity toward two gases with decreasing temperature. This phenomenon can be ascribed to two different processes that may be occurring simultaneously. One has to do with a temperature-dependent gating effect. At low enough temperatures, the window space becomes inaccessible to Xe molecules because of the lower kinetic energy of the adsorbate molecule, which cannot overcome potential barriers at the aperture of the pores that can otherwise accommodate them. These potential barriers are related to the thermal vibration of the flexible windows functioning as gates in FMOFCu. Thus, the decreasing flexibility (*via* decreasing sorbent temperature) of the windows in the porous material seems to compromise the diffusion of the larger Xe molecules inside the channels, and the kinetic effect (adsorbate diffusivity) overrides the thermodynamic effect. However, the adsorption of Kr (lighter and smaller molecule) is dominated by the thermodynamic effect; i.e., the sorbent/sorbate interaction is stronger as the temperature decreases. This

effect can be seen in Figure 8 (left) where the Xe and Kr adsorption in FMOFCu shows a distinct molecular sieving effect at temperatures below 0 ºC, where the smaller gas Kr shows larger adsorption values than the larger gas Xe. Another possibility has to do with the adsorption occurring above and below a critical temperature. Although in bulk, Xe behaves as a gas at the pressures and temperatures studied; the phase behavior can be different in a confined nano-environment (Zhao et al. 2010). Therefore, below a critical temperature, condensation at the small pore windows in FMOFCu can—in principle—occur. This prevents subsequent Xe molecules from accessing the pore channels resulting in low Xe adsorption. These two processes should not take place in FMOFZn because the cavities and windows are large enough to accommodate both gases. As a result, FMOFCu is potentially selective toward Kr over Xe at relatively moderate temperatures.

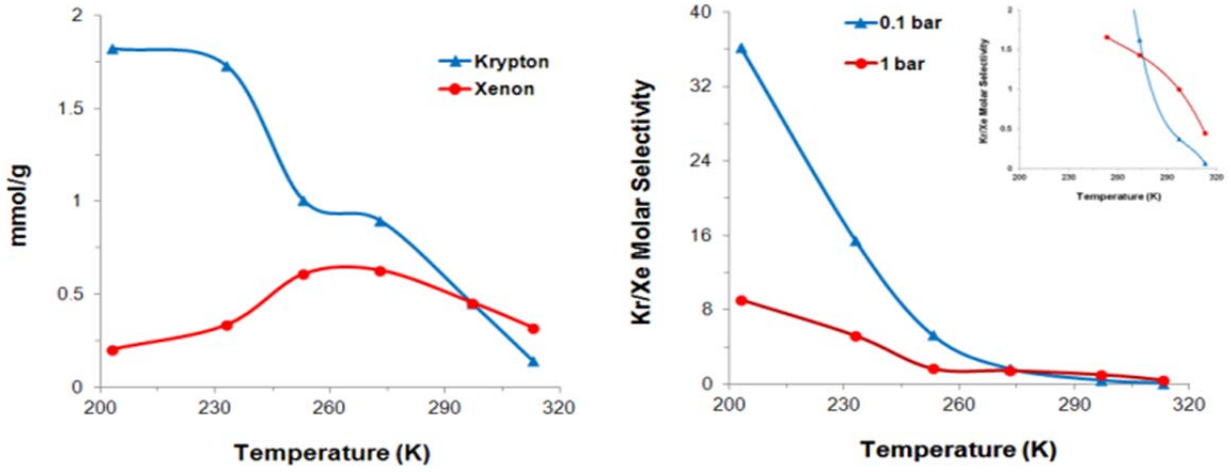

Figure 1. Adsorption of Kr and Xe as a function of temperature at 1 bar (left). The Kr/Xe selectivity in FMOFCu is inverted at 273 K (0 ºC). Estimated Kr/Xe molar selectivities from pure gas isotherms as a function of temperature at 0.1 and 1 bar (right) (inset shows a 270–313 K temperature range).

4. Cost Estimation of Metal Organic Frameworks

Synthesis cost of new synthetic materials is always a consideration for practical applications. Similar to the synthetic zeolites, MOFs are usually synthesized through hydrothermal or solvothermal reactions (see Section 3). The total cost to synthesize a MOF includes the cost of reactors, reagents, utilities, and the separation and activation of final products. The reagents usually include metal sources, organic linkers, solvents for reactions, and solvents for exchange processes. Compared to the synthetic zeolites, the cost of reactors and the cost of utilities to synthesize MOFs are assumed to be comparable. Moreover, to prepare MOFs, no additional capital investment into a totally new technology is needed. Adaptation of conventionally available precipitation and crystallization manufacturing methods is feasible. However, the cost of organic linkers and solvents to synthesize MOFs differentiate them from synthetic zeolites. Organic linkers are usually aromatic compounds that have several benzene rings in their structures with functional groups, such as carboxylic acid, hydroxyl, or amine groups. In addition, imidazole and its derivatives are also used as organic linkers to synthesize a series of MOFs, which have zeolitic structures—namely, zeolite imidazolate frameworks (ZIFs). Many organic linkers have not been commercialized on a large scale yet, having only been synthesized in research laboratories. To synthesize these special molecules is costly. The cost of organic linkers can be reduced if some new synthesis technology can be developed and adapted in the future to make use of raw petrochemicals that contain abundant aromatic compounds and minimize the use of fine chemical reagents.

To remove residual solvents remaining inside the pores and increase the surface areas and pore volumes of MOFs, solvent exchange procedures are usually used. Large amounts of organic solvents are consumed in this step and the recovery processes of the solvents are energy intensive. An alternative method to activate MOFs after synthesis is to use supercritical drying techniques. Supercritical drying methods can increase the surface areas of MOFs to even larger values than solvent exchange followed by thermal regeneration. Taking advantage of supercritical drying techniques can significantly reduce the use of solvent to activate MOFs, thus reducing the total cost to synthesize MOF materials.

To reduce the cost to synthesize per unit of MOFs, scaling up the synthesis process is a natural choice. Moreover, synthesis of MOFs in bulk is a necessity for their applications in CO_2 capture from flue gas considering the scale of the problem. The cost of raw materials required to synthesize MOFs was determined as a first step toward calculating the production cost of MOFs. Costs of the starting materials to produce some MOFs are shown and compared with some normal adsorbents in Table 1. Price quotes were obtained from multiple vendors for each raw material based on the purchase of 1 metric ton or greater quantity. Prices for individual materials were combined based on the relative amounts required for the synthesis of each MOF to arrive at the raw material cost per MOF. Examining the raw material costs is an easy first step toward estimating MOF production cost and identifies the minimum cost for a MOF. This information can be used as an early screening criterion for applications where material costs are expected to be a significant fraction of the total system cost. The BASF Corporation recently commercialized four MOF materials, including BASOLITE-A100, BASOLITE-C300 (HKUST-1), BASOLITE- Z1200 (ZIF-8), and BASOLITE-F300. The retail prices for those commercialized MOFs range from $10–$15/g (U.S. dollars), which is currently only affordable for research purposes. However, with advances in raw materials selection and synthesis technology, lower prices comparable to synthetic zeolites may be achieved for large-scale synthesis of some MOFs in the future.

Table 1. Cost of starting materials to produce MOFs (from Liu et al. 2012).

Adsorbent	Cost[(a)] (U.S. $/kg)
CuBTC (HKUST-1)	20
CoCo ($Co_3[Co(CN)_6]_2$)	35
MOF-5 (IRMOF-1)	3
Zn/DOBDC (Zn-MOF-74)	2
Ni/DOBDC (Ni-MOF-74)	6
Co/DOBDC (Co-MOF-74)	13
Mg/DOBDC (Mg-MOF-74)	1
MIL-100	16
MIL-101	5
Silica gel	1

(a) Costs were estimated from quotes obtained from multiple vendors based on the purchase of one metric ton or greater quantity and rounded to the nearest dollar.

5. Conclusions

In summary, the research team has synthesized three different MOFs (NiDOBDC, HKUST-1 and FMOFCu) that have different pore geometries and functionalities to remove the Xe and Kr from air at room temperature. All the MOFs reported in this report have high capacities of Xe (1 - 4 mmol/g) and Kr (0.9 - 2 mmol/g) at room temperature and 1 bar pressure. The uniform cylindrical pores in the

Ni/DOBDC are believed to be favorable to maximize the Xe and Kr selectivity. The Ni/DOBDC and HKUST-1can selectively adsorb Xe and Kr from air, even at ppm level concentrations. The Ni/DOBDC has a Xe capacity of 9.3 mmol/kg when the concentration of Xe is 1000 ppmv in air. More importantly, for the first time experiment results show Ni/DOBDC is able to separate 400 ppmv Xe from 40 ppmv Kr mixture in air with a Xe and Kr overall selectivity of 7.3. These results show Ni/DOBDC is a promising MOF to separate Xe from the Kr mixture at room temperature. With FMOFCu, we demonstrated—for the first time—that a MOF material can selectively capture and separate Kr from Kr and Xe mixtures at moderate temperatures. Further, bulk cost estimates indicate these materials may be economical when produced in bulk and comparable to zeolites and other porous sorbents.

The successes experienced to date clearly indicate that MOFs show some promise in separating Xe and Kr from air at near ambient temperatures, and Xe can also be separated from Kr at near ambient conditions. Although the research team has not fully investigated the range of gaseous components that might be in a process off-gas stream, the team has shown those components in breathing air do not affect Xe and Kr selectivity. Results suggest that additional MOFs can be synthesized to further enhance both capacity and selectivity.

6. References

Bazan, RE, M Bastos-Neto, A Moeller, F Dreisbach, and R Staudt. 2011. "Adsorption Equilibria of O_2, Ar, Kr and Xe on Activated Carbon and Zeolites: Single Component and Mixture Data." *Adsorption-Journal of the International Adsorption Society* 17(2):371-83. 10.1007/s10450-011-9337-3.

Bonino, F, S Chavan, JG Vitillo, E Groppo, G Agostini, C Lamberti, PDC Dietzel, C Prestipino, and S Bordiga. 2008. "Local Structure of CPO-27-Ni Metallorganic Framework Upon Dehydration and Coordination of No." *Chemistry of Materials* 20(15):4957-68. 10.1021/Cm800686k.

Eby, RS, DK Little, JR Merriman, and MJ Stephenson. 1982. Single-Column-Based Absorption Process for Treating Dissolver Off-Gas. Presented at *the Workshop on development of dissolver off-gas treatment (ERDA/050800),* 33 pp. US Energy Research and Development, Washington, DC.

Eddaoudi, M, J Kim, N Rosi, D Vodak, J Wachter, M O'Keeffe, and OM Yaghi. 2002. "Systematic Design of Pore Size and Functionality in Isoreticular MOFs and Their Application in Methane Storage." *Science* 295(5554):469-72.

Farha, OK and JT Hupp. 2010. "Rational Design, Synthesis, Purification, and Activation of Metal-Organic Framework Materials." *Accounts of Chemical Research* 43(8):1166-75. 10.1021/Ar1000617.

Greathouse, JA, TL Kinnibrugh, and MD Allendorf. 2009. "Adsorption and Separation of Noble Gases by IRMOF-1: Grand Canonical Monte Carlo Simulations." *Industrial & Engineering Chemistry Research* 48(7):3425-31. 10.1021/ie801294n.

Henrich, E and F Weirich. 1989. Development of a Cryogenic Absorption Process for Rare Gas Removal from Reprocessing Off-Gas. Presented at *the 16th DOE Nuclear Air Cleaning Conference (CONF-801038),* US Department of Energy, Washington, DC.

Jameson, CJ, AK Jameson, and HM Lim. 1997. "Competitive Adsorption of Xenon and Krypton in Zeolite NaA: Xe-129 Nuclear Magnetic Resonance Studies and Grand Canonical Monte Carlo Simulations." *Journal of Chemical Physics* 107(11):4364-72. 10.1063/1.474778.

Liu, J, PK Thallapally, BP McGrail, DR Brown, and J Liu. 2012. "Progress in Adsorption-Based CO_2 Capture by Metal-Organic Frameworks." *Chemical Society Reviews* 41(6):2308-22. 10.1039/C1cs15221a.

Liu, JT, J.; Thallapally, P. K.; McGrail, B. P. 2012. "Selective Adsorption of CO_2 from Flue Gases - Fixed Bed Approach." *J. Phys. Chem. C* 116:9575–81.

Mueller, U, M Schubert, F Teich, H Puetter, K Schierle-Arndt, and J Pastre. 2006. "Metal-Organic Frameworks - Prospective Industrial Applications." *Journal of Materials Chemistry* 16(7):626-36.

Munakata, K, S Kanjo, S Yamatsuki, A Koga, and D Ianovski. 2003. "Adsorption of Noble Gases on Silver-Mordenite." *Journal of Nuclear Science and Technology* 40(9):695-97.

Perry, JJ, JA Perman, and MJ Zaworotko. 2009. "Design and Synthesis of Metal-Organic Frameworks Using Metal-Organic Polyhedra as Supermolecular Building Blocks." *Chemical Society Reviews* 38(5):1400-17. 10.1039/B807086p.

Ryan, P, OK Farha, LJ Broadbelt, and RQ Snurr. 2011. "Computational Screening of Metal-Organic Frameworks for Xenon/Krypton Separation." *Aiche Journal* 57(7):1759-66. 10.1002/aic.12397.

Sanchez, C, KJ Shea, and S Kitagawa. 2011. "Recent Progress in Hybrid Materials Science." *Chemical Society Reviews* 40(2):471-72. 10.1039/C1cs90001c.

Thallapally, PK, JW Grate, and RK Motkuri. 2012. "Facile Xenon Capture and Release at Room Temperature Using a Metal-Organic Framework: A Comparison with Activated Charcoal." *Chemical Communications* 48(3):347-49. 10.1039/C1cc14685h.

Zhao, D, DQ Yuan, R Krishna, JM van Baten, and HC Zhou. 2010. "Thermosensitive Gating Effect and Selective Gas Adsorption in a Porous Coordination Nanocage." *Chemical Communications* 46(39):7352-54. 10.1039/C0cc02771e.

Appendix A

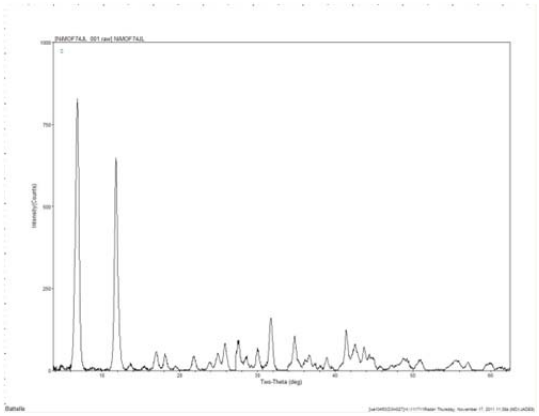

Figure 9. X-ray diffraction patterns for the Ni/DOBDC.

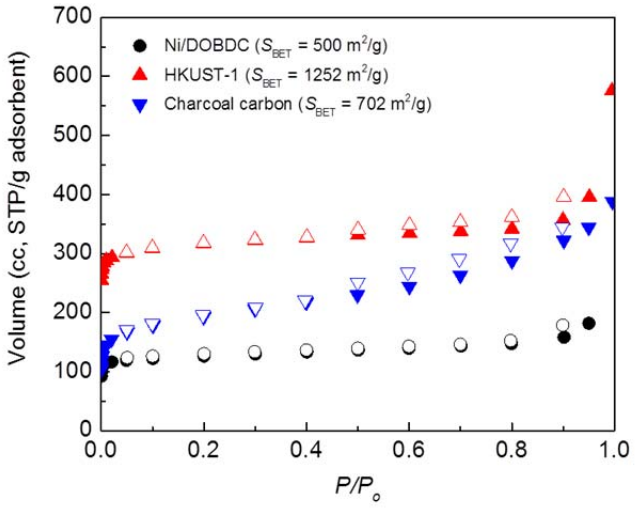

Figure 2. Isotherms (BET) for the Ni/DOBDC, HKUST-1, and charcoal carbon pellets. Filled symbols are adsorption data and unfilled are desorption data.

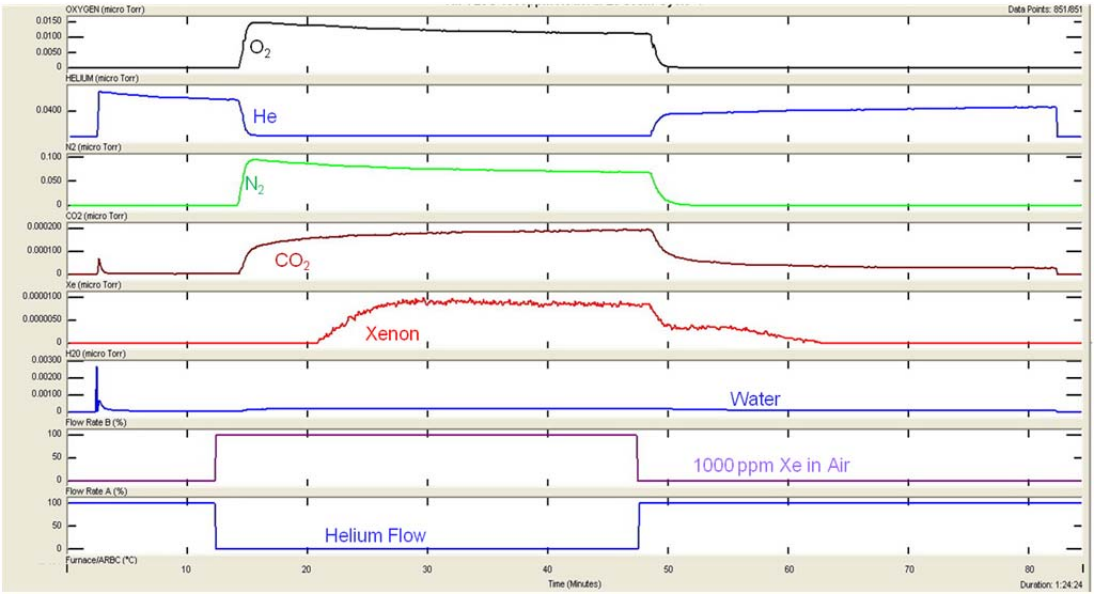

Figure 11. A Graph showing all component breakthrough curves for the Ni/DOBDC with 1000 ppmv Xe in air at 100 kPa and 25 °C.